Excitatory and inhibitory interaction fields of flankers revealed by contrast-masking functions

Chien-Chung Chen

Department of Psychology, National Taiwan University, Taipei, Taiwan

Christopher W. Tyler

The Smith-Kettlewell Eye Research Institute, San Francisco, CA, USA

To study spatial interactions corresponding to the non-classical receptive field organization for human vision, we used a dual-masking paradigm to measure how target contrast discrimination can be affected by the relative location of the flankers. The observers' task was to detect a 4 cycle/deg vertical Gabor superimposed on a matching Gabor pedestal in the presence of vertical Gabor flankers. The flankers were either (i) collinear with the target and varying in distance or (ii) at a fixed distance from the target but with varying in location relative to the vertical axis. Compared with the no-flanker condition, the collinear flankers *decreased* target threshold at low pedestal contrasts (facilitation) and *increased* threshold at high contrasts (suppression). The low contrast facilitation increased with distance up to 4 wavelengths and decreased beyond that. Both facilitative and suppressive flanker effects were greatest at the collinear location and decreased monotonically as flanker location deviated from the collinear axis. These flanker effects are modeled with our sensitivity modulation model, which suggests that the flanker effects are multiplicative terms applied to both the excitatory and inhibitory terms of a divisive inhibition response function. The model parameters show that the facilitative flanker effect is narrowly tuned in space. The data are not compatible with a model of additive normalization by the pedestal contrast or with the uncertainty model.

Keywords: lateral interaction, contrast discrimination, masking, sensitivity modulation, TvC function

Citation: Chen, C., & Tyler, C. W. (2008). Excitatory and inhibitory interaction fields of flankers revealed by contrast-masking functions. *Journal of Vision, 8*(4):10, 1–14, http://journalofvision.org/8/4/10/, doi:10.1167/8.4.10.

Introduction

The visual processing of a stimulus projecting to one location on the retina can be modified by the presence of other stimuli at different locations. By measuring detection thresholds for a target Gabor pattern at the fovea flanked by two other high-contrast Gabor patterns (flankers), Polat and Sagi (1993, 1994) reported that the target threshold decreased from the absolute threshold when a pair of collinear flankers (with their stripes collinear with those in the target) was presented (facilitation). Similar flanker facilitation effects were also reported by Chen and Tyler (2001, 2002), Solomon, Watson, and Morgan (1999), and Zenger and Sagi (1996).

The amount of flanker facilitation varies with the distance between the flankers. Polat and Sagi (1993, 1994) showed that the facilitation is greatest when the distance between the target, and the flanker was about three times the wavelength the target carrier wave. The facilitation effect reduced as the distance either increased or decreased from the maximal facilitation point. This result quantifies the distance tuning of the flanker effect. The location of the flanker related to the target also affects the flanker facilitation. Compared with Gabor flankers with their stripes collinear with the target, flankers at the sides of the targets, hence with their stripes parallel to those of the target, produced less facilitation (Polat, Sagi, & Norcia, 1997).

The location-specific flanker effect is consistent with the single cell recording result on V1 cells. Mizobe, Polat, Pettet, and Kasamatsu (2001) showed that not only can the contrast response function of a V1 neuron to a target within its classical receptive field be modulated by flankers outside its classical receptive field, but also that the amount and the form of modulation are dependent on the relative distance between the target and the flankers. Kapadia, Westheimer, and Gilbert (2000) showed that while collinear flankers facilitated the responses of a V1 neuron to a target of preferred orientation within its classical receptive field, flankers on the side of the target suppressed its responses. Hence, not only do stimuli outside the classical receptive field of a neuron still have influence of the cell responses to stimuli within it, but also this influence depends on the relative location of the flankers to the classical receptive fields. This phenomenon gives rise to the now-widespread concept of the non-classic receptive field (Cavanaugh, Bair, & Movshon, 2002; Freeman, Ohzawa, & Walker, 2001).

Current studies on lateral context effects focus on the facilitation of a target mechanism produced by flanking stimuli. This facilitative effect may not reveal the

doi: 10.1167/8.4.10 Received July 6, 2007; published April 17, 2008 ISSN 1534-7362

complete picture of the lateral context effect, however. Both psychophysical (Chen & Tyler, 2001, 2002) and neurophysiological (Chen, Kasamatsu, Polat, & Norcia, 2001; Polat et al., 1997; Sengpiel, Baddeley, Freeman, Harrad, & Blakemore, 1998) evidence show that even the same collinear flankers at the same location can have different effects on the response to the target as its contrast is varied. Polat et al. (1997; see also Chen et al., 2001) measured the flanker effect on the responses of striate cortical neurons to target Gabor patches located within their classical receptive fields. In a large number of cells for which the flankers themselves produced no response, the responses increased at low contrast and decreased the responses at high contrast in the presence of the flankers. That is, depending on the target contrast, the same flanker could have either facilitative or suppressive effect on a given cell response. The facilitation at low target contrast is consistent with the flanker effect reported by Polat and Sagi (1993). The high contrast suppression, however, cannot be revealed psychophysically with the detection paradigm.

Chen and Tyler (2000, 2001) explored the corresponding effects psychophysically with a dual-masking paradigm in which the observer had to detect a target superimposed on a pedestal (primary mask) in the presence of two collinear flankers (secondary mask). Detection of a target superimposed on a pedestal, called a masking experiment in the literature, has been a well-established paradigm for studying the visual detection mechanisms (Breitmeyer, 1984; Chen & Foley, 2004; Foley, 1994; Foley & Chen, 1999; Kontsevich & Tyler, 1999a; Legge & Foley, 1980; Meese & Holmes, 2007; Ross & Speed, 1991; Wilson, McFarlane, & Philips, 1983). If the target and the pedestal are the same in all spatiotemporal parameters except contrast, as in Chen and Tyler (2000, 2001), this experiment is equivalent to contrast discrimination. Without flankers, the target threshold vs. pedestal contrast (TvC) function has a dipper shape: Relative to the detection threshold measured with no pedestal, the target threshold first decreases (facilitation) and then increases as the pedestal contrast is increased. When flankers are present, they can facilitate target detection at zero pedestal contrast as reported by previous authors (Polat & Sagi, 1993, 1994; Solomon et al., 1999; Zenger & Sagi, 1996). However, the amount of lateral facilitation decreases as the pedestal contrast is increased. Thus, compared with the no flanker condition, the TvC function for the flanker condition shows a shallower dip. As the pedestal contrast further increases, the target threshold for flanker condition rises above the target threshold for the no-flanker condition. As a result, the flanker and the no-flanker TvC functions show a cross-over phenomenon: The flanker TvC function has lower thresholds at low pedestal contrasts and higher thresholds at high contrast. This result is consistent with the behavior of striate cortical neurons. Subsequently, Adini and Sagi (2001) and Zenger-Landbolt and Koch (2001) also reported similar phenomena.

The dual-masking paradigm offers a means of studying the spatial characteristics of the flanker effect on contrast discrimination. It provides much information not available with the traditional lateral-masking paradigm (e.g., Polat & Sagi, 1993) for the study of the lateral effect on detection. In particular, we employed the dual-masking paradigm to investigate the location specificity of the lateral effect. Since flanker stimuli can have both facilitatory and masking effects on the target mechanism, a reduction of lateral facilitation by a side flanker can be seen as either a decrease in facilitation or an increase in masking. We attempt to resolve this distinction by comparing how the TvC functions change with the relative distance and location of the flankers and by fitting the data to a quantitative model to observing how model parameters change with the flanker position. In a sense, our experiment is the psychophysical equivalent of mapping the non-classical receptive field of the target detection mechanisms.

Methods

Stimuli

The target, pedestal, and flankers were all Gabor patches defined by the equation

$$G(x,y;c,u_x,u_y) = B + B{*}c{*}\cos(2\pi fx){*}\exp(-(x-u_x)^2/2\sigma^2) * \exp(-(y-u_y)^2/2\sigma^2), \quad (1)$$

where B was the mean luminance, c was the contrast of the pattern ranging from 0 to 1, f was the spatial frequency, σ was the scale parameter (standard deviation) of the Gaussian envelope, and u_x and u_y were the horizontal and the vertical displacements of the pattern, respectively. All patterns had a spatial frequency (f) of 4 cycles per degree and a scale parameter (σ) of 0.1768°. The target and the pedestal were vertically oriented. The contrasts of the flankers (c) were −6 dB or 0.5. The target and the pedestal were centered at the fixation point; hence, their displacement u_y was zero. Figure 1 illustrates the arrangement of flankers in different test conditions.

In the distance condition, the two flankers were placed above and below the target with displacements (u_y) of 0.35°, 0.71°, 1.06°, 1.41°, and 2.12°, corresponding to 1.4, 2.8, 4.2, 5.6, and 8.4 times target carrier wavelength. In the azimuth condition, the center of the flankers was always 0.71° away from the center of the target but were placed at orientations of 11° (for observer CC only), 22°, 30°, 45°, and 90° away from the vertical axis. Hence, u_x was parameterized as 0.71°*sin(θ) and u_y as 0.71°*cos(θ), with θ being the azimuth or the angular deviation from the

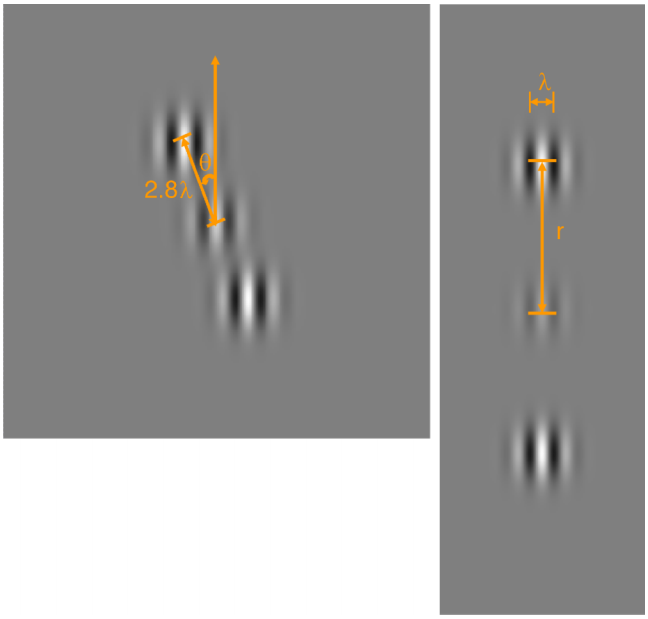

Figure 1. Arrangement of the Gabor target and the Gabor flankers in (A) azimuth and (B) distance conditions.

vertical axis. All stimuli were presented concurrently. The temporal waveform of the stimuli was a 90-ms rectangular pulse.

Procedures

We used a temporal two-interval forced-choice (2IFC) paradigm to measure the target threshold. On each trial, both the pedestal and the flankers were presented in both intervals. The target task of the observer was to determine which interval contained the target, which was presented randomly in either of the intervals. We used the Ψ threshold-seeking algorithm (Kontsevich & Tyler, 1999b) to measure the threshold at 75% correct response level. There were 40 trials for each threshold measurement. Each datum point reported was an average of 4 to 8 repeated measures. We randomized the sequence in which pedestal contrast and flanker distance and location were presented in each threshold measurement.

Three observers participated in this study. CC is an author of this paper, and SS and SW were paid observers naive to the purpose of the study. All observers had corrected to normal (20/20) visual acuity.

Apparatus

The stimuli were presented on two Mitsubishi Diamond Scan 15-in. monitors each driven by an IXMicro in3D ProRez graphic board. A Macintosh computer controlled the graphic boards. Lights from the two monitors were combined by a beam splitter. This two-monitor setup allowed us to present the target on one monitor and the context (the pedestal and the flankers) on the other. This arrangement gave us the advantage of independent control of the contrast of the target while ensuring that the context was the same in two intervals of a trial. The viewing field was 10.7° (H) by 8° (V). The resolution of the monitors was 640 horizontal by 480 vertical pixels, giving 60 pixel per degree at the viewing distance used (128 cm). The refresh rate of the monitor was 66 Hz. We used the LightMouse photometer (Tyler & McBride, 1997) to measure the full-detailed input–output intensity function of the monitor. This information allowed us to compute linear lookup table settings to linearize the output within 0.2%. The mean luminance of the display was set at 19 cd/m^2.

Results

Figure 2 shows the target threshold vs. pedestal contrast (TvC) functions for flankers at different azimuth (specified in polar coordinates). Each row in Figure 2 shows the data of one observer. The left column shows TvC functions for flankers deviating from the collinear axis by 0° to 22° (panels A, C, and E) and the right column for 45° to 90° (panels B, D, and F). The no-flanker TvC functions are plotted in both top and bottom panels of the respective subjects for reference. The smooth curves in each panel are the fits of the sensitivity modulation model discussed later.

Without flankers, the TvC function showed a classic dipper shape: The threshold first decreased and then increased as the pedestal contrast was increased. The greatest threshold reduction occurred when the pedestal contrast was at about its own detection threshold. This dipper-shaped TvC function is well established (Chen & Foley, 2004; Foley, 1994; Kontsevich & Tyler, 1999a; Legge & Foley, 1980; Ross & Speed, 1991). When the collinear flankers were presented, they had two major effects on the TvC functions. First, without the pedestal (denoted as the $-\infty$ dB contrast pedestal condition in the figures), the flankers had the facilitatory effect of reducing the target detection threshold by 3–6 dB (30–50% decrease in linear contrast). This result is comparable with that reported by Polat and Sagi (1993, 1994) in a similar condition. Second, the flankers at high pedestal contrasts increased target threshold by as much as 6 dB (or about a 100% increase in terms of linear contrast). This threshold increment was similar for all measured pedestal contrasts above −18 dB. The combined effect of all these changes can be viewed as shifting the TvC function horizontally to the left by up to 6 dB, as is modeled by uniform shifts in the fitted model function. It is important to emphasize that this effect was always a

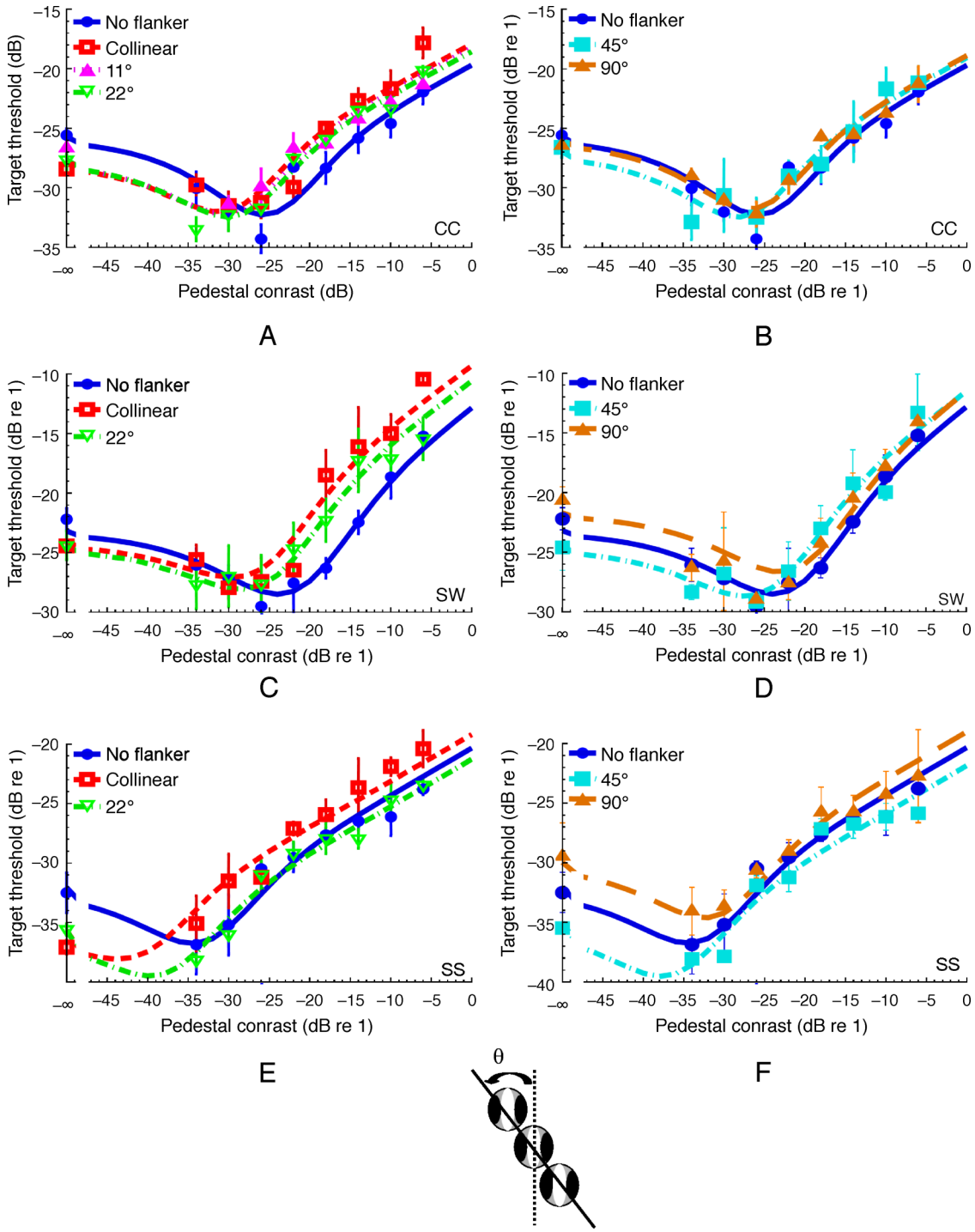

Figure 2. The target threshold vs. pedestal contrast (TvC) functions in the presence of flankers at different azimuths (deviation from collinear axis, θ) from 0° (collinear) to 90°. The left column (A, C, E) is for small θ while the right column (B, D, F) is for large θ. The no-flanker TvC functions are plotted in each panel (blue solid curves) as a reference. Each row illustrates TvC functions for one observer. The smooth curves in each panel are the fits of the sensitivity modulation model. See keys for the meaning of the symbols. Note that the flankers tend to facilitate visibility at low pedestal contrasts but impair it at high pedestal contrasts.

parallel shift; up to the highest pedestal contrast we measured, the measured TvC functions show no sign of convergence. These effects are consistent with those previously reported with different observers (Chen & Tyler, 2001, 2002). Both effects reduced as the flanker deviated from the collinear axis. As a result, the TvC functions were closer to that of the no-flanker condition vs. flanker azimuth.

Figure 3 shows the flanker azimuth effect on target contrast detection measured as the target threshold at zero

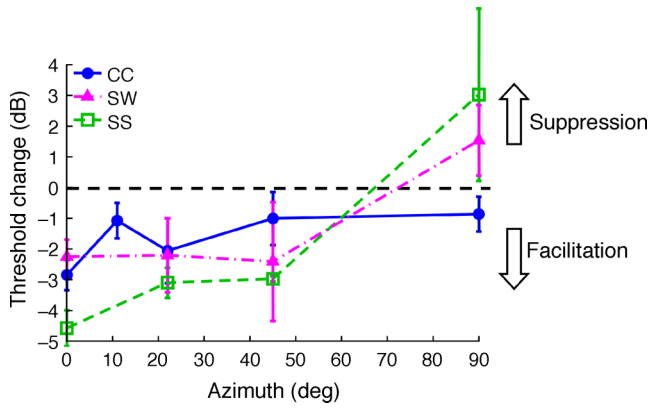

Figure 3. Variation of the target detection threshold (measured without pedestal) with the deviation of the flankers from the collinear axis for three observers: CC (blue), SW (magenta), and SS (green). Note that the facilitatory effect of the flankers has a broad location tuning over azimuth.

pedestal contrast. Moving the flanker off the collinear axis by a small amount (up to 22° for CCC and 45° for SAS and SW) had little effect on the flanker facilitation for detection. The flanker facilitation for detection disappeared when the flankers were at the sides of the target (90° off collinear axis), as reported by Solomon and Morgan (2000) and Yu, Klein, and Levi (2002). The off-axis flankers had less threshold elevation effect at high pedestal contrasts than the collinear flankers. As a result, the off-axis TvC functions at high contrasts fall below those for collinear flankers. In general, the target threshold elevation effect at high pedestal contrasts decreased with the flankers deviated from the collinear axis.

Figure 4 shows the flanker distance effect on the full TvC functions. The TvC functions for flankers at 2.8 λ in Figure 4 are the same as the collinear TvC functions in Figure 2 for the respective observers. This and the no-flanker conditions are plotted here again for reference. The target threshold at the 1.4 λ flankers was apparently dominated by the flankers acting as a pedestal and was practically constant for the measured pedestal contrasts. The masking effect at high pedestal contrast was observed at the 2.8 λ to 4.2 λ conditions. However, there it was unclear whether the flanker effect persisted at high pedestal contrasts for long distance (>5.6 λ) flankers.

Figure 5 shows the flanker distance effect on the detection thresholds. At 1.4 λ, the flankers elevated the target detection threshold in the zero pedestal condition by 6–9 dB (a 2- to 3-fold increase). Based on the proximity between the flankers and the targets, this pronounced masking effect may be due to the overlap between the receptive field of the target detector and the flankers. As a result, the flankers also acted as a pedestal to cause strong threshold elevation. Conversely, the 2.8 λ to 5.6 λ flankers produced pronounced facilitation for target detection at no pedestal. Two of the observers (SS and SW) even showed a robust *facilitation* for the 8.4 λ flanker condition. The distance effect on target detection was consistent with previous reports (Polat & Sagi, 1993).

Discussion

The neural sensitivity modulation model

The neural sensitivity modulation model is a conceptual framework for spatial contrast interactions that has successfully accounted for psychophysical and neurophysiological data (Chen & Kasamatsu, 1998; Chen et al., 2001, Chen & Tyler, 2000, 2001). This model proposes two different inter-mechanism interactions, as diagramed in Figure 6. Within each hypercolumn, the mechanism response is assumed to have the typical influence from other neural mechanisms in the same hypercolumn through contrast normalization or divisive inhibition (shown within the dashed box). Between hypercolumns (or other local subdivisions), however, the neural interaction is in the form of a lateral sensitivity modulation (shown outside the dashed-outline box in Figure 6), which modulates the sensitivity of both the local detection mechanism and the distributed mechanisms forming the divisive inhibitory pool. The original version of this model was developed to explain the variety of flanker effects on response functions of striate cortical cells (Chen & Kasamatsu, 1998; Chen et al., 2001), and the same mathematical form was later shown to explain the psychophysical data as well (Chen & Tyler, 2001). In particular, this model can account for the paradoxical result that the lateral effects increase with target contrast even though the flanker contrast remains constant (Polat et al., 1997) while conventional contrast normalization models (e.g., Heeger, 1992) cannot. Cavanaugh et al. (2002), Freeman et al. (2001), Meese, Summers, Holmes, and Wallis (2007), Xing and Heeger (2001), and Yu, Klein, and Levi (2003) have subsequently proposed models of a similar form to account for lateral interaction effects.

The first stage of each local mechanism j is a linear operator within a spatial sensitivity profile $f_j(x, y)$. The excitation of this linear operator to an image $g(x, y)$ is given as

$$E_j' = \Sigma_x \Sigma_y f_j(x, y) \bullet g(x, y), \quad (2)$$

where the linear filter $f_j(x, y)$ is defined by a Gabor function (see Methods section). (It is assumed that we are concerned with the output of the neural mechanism located for maximal activation by the image, i.e., that $E_j' = \max [E_j'(x', y')]$ across the visual field.) If the image

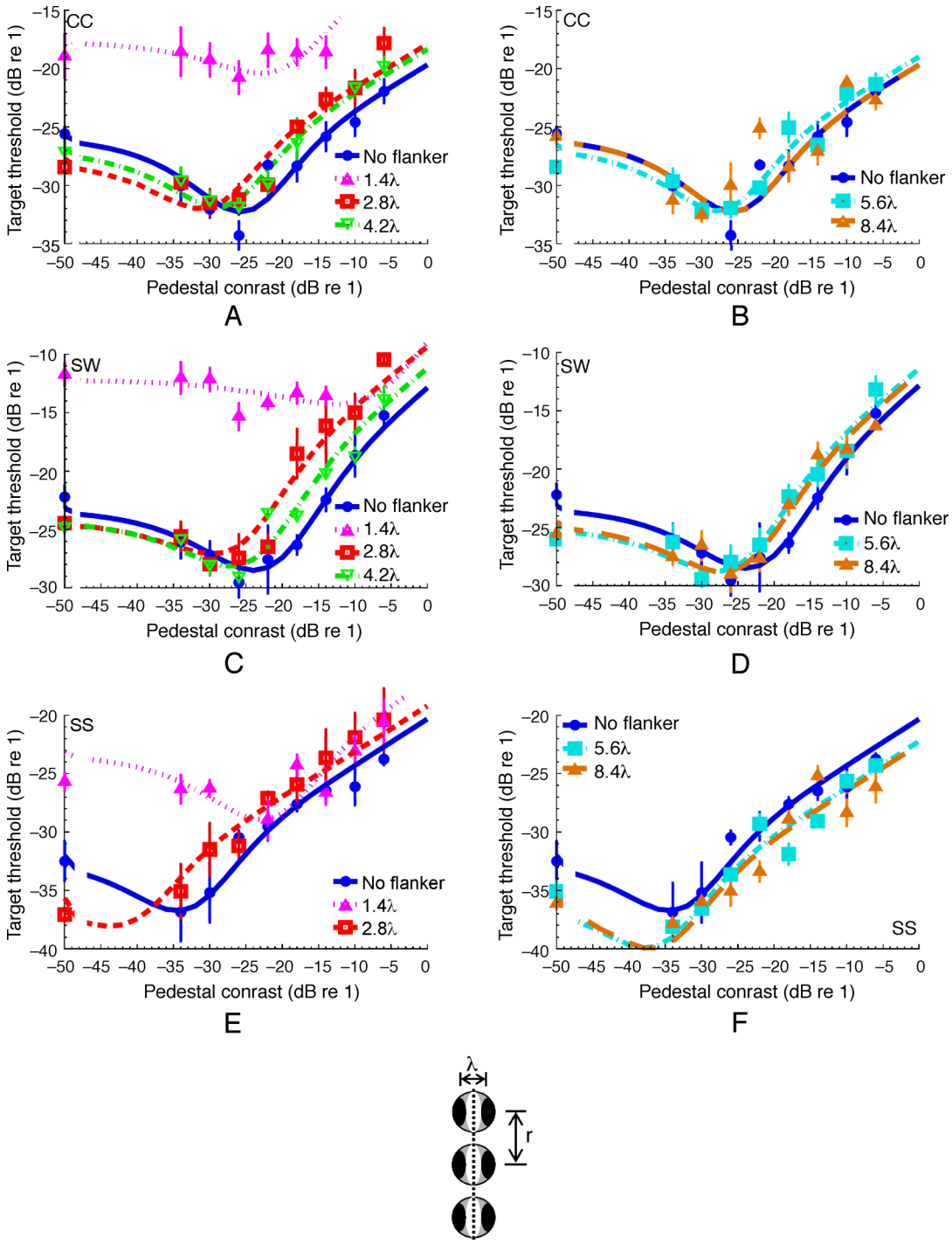

Figure 4. The target threshold vs. pedestal contrast (TvC) functions in the presence of flankers at different distance. The left column (A, C, E) is for small distances (1.4–4.2 wavelength units) while the right column (B, D, F) is for large distances (5.6–8.4. wavelength unit). The no-flanker TvC functions are plotted in each panel (blue curve) as a reference. Each row illustrates TvC functions for one observer. The smooth curves in each panel are the fits of the sensitivity modulation model. See keys for the meaning of the symbols. Note that flanker distance has complex effects on the TvC function.

$g(x, y)$ is a periodic pattern with contrast c, as was used in our experiment, Equation 2 can be simplified to

$$E_j' = S_{ej} \bullet c, \qquad (2')$$

where S_{ej} is a constant defining the excitatory sensitivity of the mechanism. The detailed derivation of Equation 2′ from Equation 2 has been discussed elsewhere (Chen, Foley, & Brainard, 2000).

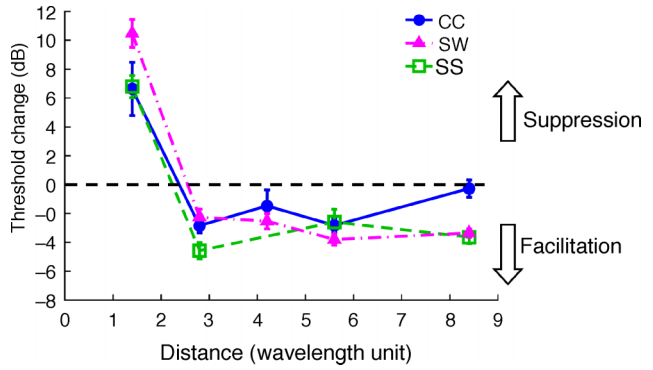

Figure 5. The target detection threshold changes with the distance between the flankers and the target for three observers: CC (blue), SW (magenta), and SS (green). Note the extended range of facilitation (>6 λ), replicating the results of Polat and Sagi (1993).

The excitation of the linear operator is halfwave rectified (Chen & Tyler, 1999; Foley, 1994; Foley & Chen, 1999; Teo & Heeger, 1994) to produce the rectified excitation E_j

$$E_j = \max(E_j^{'}, 0), \tag{3}$$

where max denotes the operation of choosing the greater of the two numbers.

If there is no flanker present, the response of the jth mechanism is given by its rectified excitation raised to the power p and then divided by a divisive inhibition term I, limited at low levels by an additive constant z. That is,

$$R_j = E_j^p/(I_j + z). \tag{4}$$

The divisive inhibition input is a non-linear combination of the rectified excitations of all relevant mechanisms, that is, those have non-zero response to the stimuli, within the same hypercolumn, given by

$$I_j = \Sigma_n w_n E_n^q = \mathrm{Si}_j \bullet c^q, \tag{5}$$

where $Si_j = \Sigma_n(w_n Se_j^q)$ is the sensitivity of the jth mechanism to the divisive inhibition input.

In the absence of the flankers, this model has the same form as other divisive inhibition or contrast normalization models (Foley, 1994; Ross & Speed, 1991; Teo & Heeger, 1994; Watson & Solomon, 1997; Wilson & Humanski, 1993). When the flankers are presented and produce responses in the flanking mechanisms, however, our model includes the critical assumption that these mechanisms send a lateral signal that modulates the sensitivity of both the excitatory and the divisive inhibitory inputs to the target mechanism. Let Ke and Ki denote the sensitivity modulation factors to the excitatory and the inhibitory inputs, respectively. Therefore, the response function in the presence of flankers becomes

$$R_j^{'} = (\mathrm{Ke} \bullet E_j^p)/(\mathrm{Ki} \bullet I_j + z). \tag{6}$$

Both Ke and Ki are functions of flanker contrast. However, in the experiment reported in this paper, only two flanker contrasts (0% and 50%) were used. Therefore, we simply take Ke and Ki to have the value of 1 when the flanker contrast is 0 (thus reducing Equation 6 to Equation 4) and to be free parameters to be estimated when the flanker contrast is 50%. Both Ke and Ki are required in order to account for different aspects of the flanker effect (Chen & Tyler, 2001). In our two-interval forced-choice experiment, when there are no flankers, the difference in response is given as

$$D = R_{j,b+t} - R_{j,b}, \tag{7}$$

where j is the mechanism that gives the greatest response difference, b denotes the pedestal contrast, and $b + t$ denotes the target-plus-pedestal contrast. The target reaches the threshold when its contrast increases by a certain amount (Legge & Foley, 1980), designated as 1 in our model fitting. When the flanker is presented, we simply replace R_j (Equation 4) by R_j' (Equation 6) in Equation 7.

To reduce the number of free parameters in the model, we applied the following constraints on the parameter values: (1) All response function parameters, p, q, and z, were the same for all conditions in each observer. (2) The sensitivity parameter (S_e) to the target was set at 100. (3) The contribution of the flanker to the sensitivity parameters (S_e and S_i) was set to 0 for all flankers that were more than one wavelength unit away

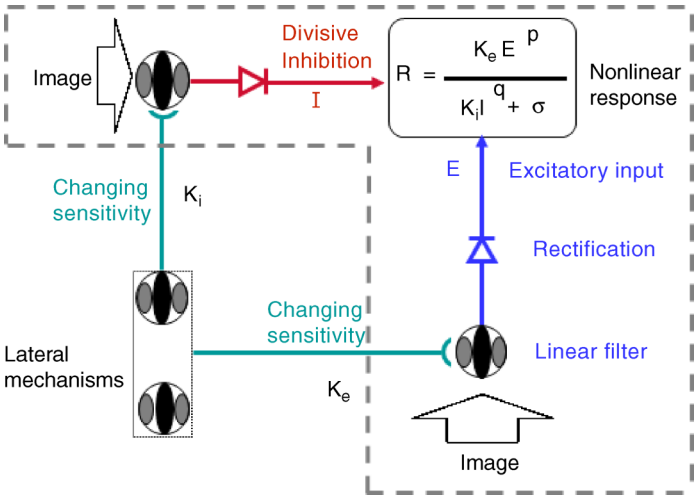

Figure 6. A diagram of the sensitivity modulation model we used to fit the data. Dashed line encloses local mechanisms. See text for details.

from the target; and (4) the lateral effect parameters Ke and Ki were set to 1 in the pedestal only conditions.

The fit of this model is shown as smooth curves in Figures 2 and 4. The overall goodness-of-fit of the model, represented as the root mean squared error (RMSE) to the full data set, was 1.19 dB for CCC, 1.08 dB for SS, and 1.13 dB for SW. These values are close to the mean standard deviation of the measurement error (1.02 dB for CCC, 0.99 dB for SS, and 1.40 dB for SW). Put another way, the model accounts of 86%, 90%, and 92% of the variance of the data for the three subjects, respectively. Hence, the model gives an excellent description of the data in all cases.

Space tuning

Figure 7 shows how lateral modulation parameters Ke and Ki changed with the azimuth of the flankers. The azimuth effect is assumed to be a cosine function because the flanker at azimuth $\theta°$ is the same as the flanker at $\theta + 180°$ and is assumed to have the same effect as the flanker at $-\theta°$ (symmetry about collinear axis) and $\theta + 180°$ (symmetry about orthogonal axis). That is,

$$K_m = 1 + (a_m' + b_m' * \cos(2\theta)), \quad (8)$$

where a_m and b_m are free parameters, and m is either e or i to denote excitatory and inhibitory modulation parameters. As shown below, the value of parameter b_m' also depends on the distance of the flankers The fit of this equation is shown in Figure 6 as smooth curves. The bandwidth of the tuning function, measured as the half height point, was at 46°–48° for both Ke and Ki, all observers. This result is comparable with the estimation of perceptual field by Ledgeway, Hess, and Geisler (2005) with a contour integration paradigm. There is very little, if any, individual difference on the azimuth tunings.

The distance tuning of the lateral modulation parameters Ke and Ki is shown in Figure 8. We chose to fit a log gamma function to these parameters. That is,

$$K_m = 1 + b_m'' * \mathrm{lt}^{(c_m - 1)} * \exp(\mathrm{lt}/d_m) \quad (9)$$

and

$$\mathrm{lt} = \log_{10}(t), \quad (10)$$

where t denotes the distance between the target and the flanker, and b_m'', c_m, and d_m are free parameters. The excitatory parameter Ke peaks between 2.1 and 3.5 λ (where λ is the target wavelength). Previous lateral-masking studies reported that flankers produced the maximum facilitation effect on target detection when the distance between the target and the flankers was about 3 λ (Polat & Sagi, 1993; Solomon et al. 1999). Since the lateral effect on detection is dominated by the excitatory

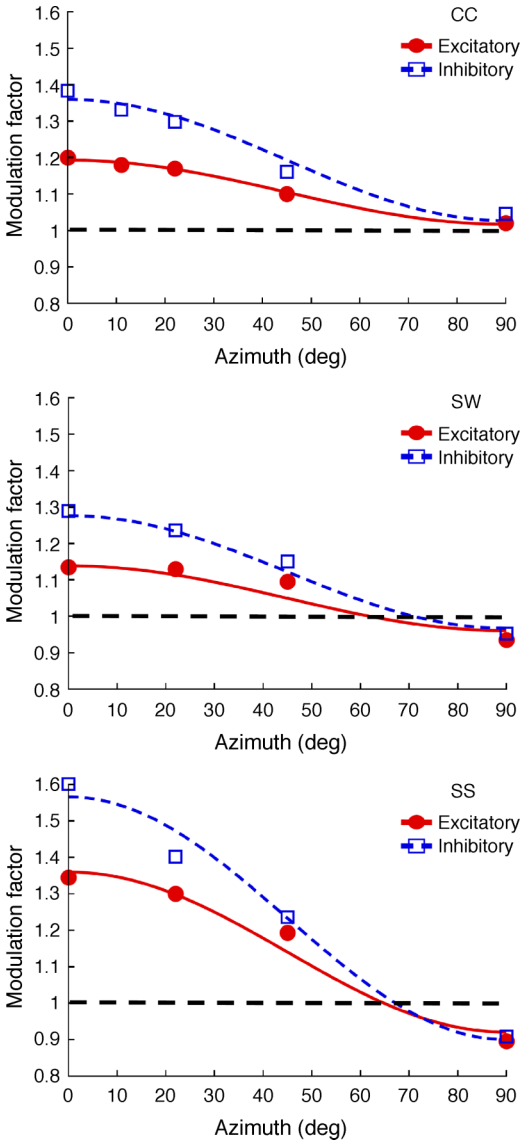

Figure 7. The excitatory (red) and the inhibitory (blue) sensitivity parameters as a function of flanker azimuth. The smooth curves were fits of Equation 8.

parameter (Chen & Tyler, 2001), our result explains such distance effects in lateral masking. The inhibitory parameter Ki peaks between 1.9 and 2.8 λ, closer than Ke. In contrast with the *azimuth* tuning, which also shows a great consistency among observers, the bandwidth of the *distance* tuning function showed notable individual differences. The half-height distance was about 1.2 λ for Ke and Ki across all observers at the near end (closer to the target) but ranged from 4 to 8 λ at the far end.

Combining Equations 8 and 9 therefore, we have a complete description of co-orientation lateral effects in the space surrounding the target, that is,

$$K_m = 1 + b_m * (a_m + \cos(2\theta)) * (\mathrm{lt}^{(c_m - 1)} * \exp(\mathrm{lt}/d_m)), \quad (11)$$

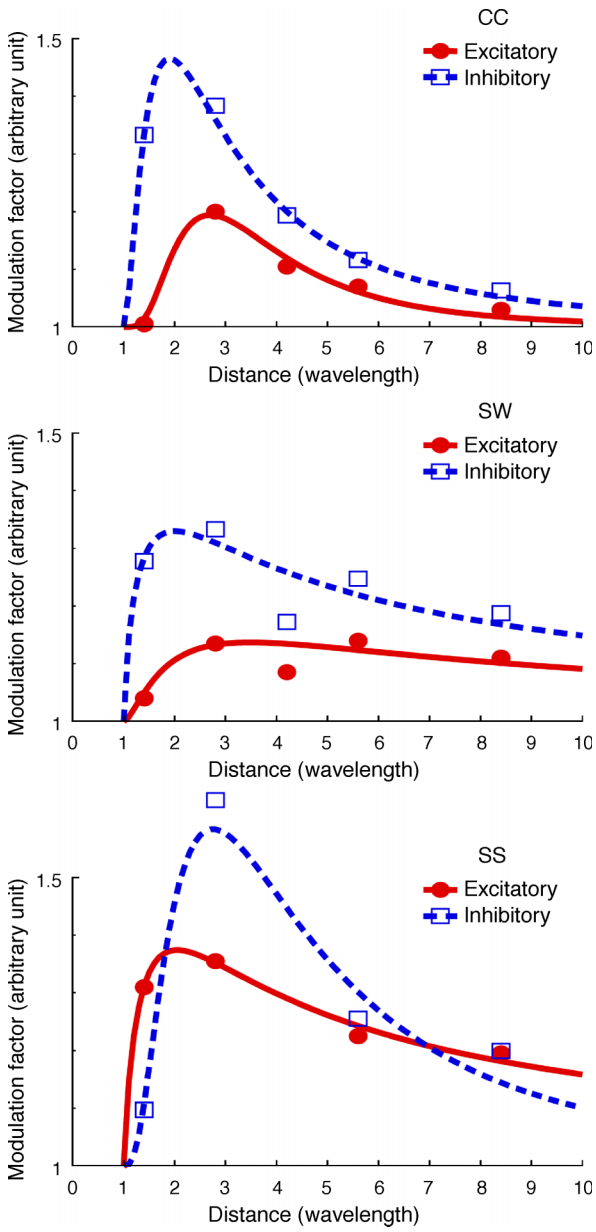

Figure 8. Variation of the excitatory (red) and inhibitory (blue) sensitivity parameters as a function of the distance between the flanker and the target. The smooth curves are fits of Equation 9.

where $a_m = a'_m / b'_m$. We may then plug the parameter values from Equation 11 back into Equation 6 to estimate how the response of the target detector changes with the spatial location of the flanker, which is the "non-classical receptive field" (NCRF) of the target detector. As depicted in the pseudocolor plots of Figure 9, the NCRF is contrast dependent. The low contrast NCRF showed an extended excitatory region near the collinear axis of the target detector while the high contrast NCRF showed an inhibitory region along the same axis.

This result is consistent with the contrast-dependent size tuning reported in the single-cell recording literature (Cavanaugh et al., 2002; Kapadia, Westheimer, & Gilbert, 1999). That is, the response of a V1 cells increases with the size of a local stimulus projected onto its receptive field only up to a certain extent and then the response decreases as with further size increases. On the other hand, the response to a low contrast stimulus keeps increasing with stimulus size and shows little size-dependent suppression. In our context, the high contrast NCRF showed an inhibitory region beyond the target area (Figure 9, right). A high contrast target large enough to cover this inhibitory region should induce an inhibitory lateral interaction on the target detection mechanisms. This effect is consistent with the reduction of cell response for large stimuli observed in the single cell recording literature. On the other hand, the low contrast NCRF region showed an extended excitatory region (Figure 9, left). Hence, a low contrast target large enough to cover this region should induce an excitatory lateral interaction on the target detection mechanisms. Increasing the target size will also increase the response of the target detector. This effect, again, is consistent with the size effects observed in the single-cell recording literature.

Pedestal effect and flanker effect

It is suggested (e.g., Solomon et al., 1999) that flanker facilitation (Polat & Sagi, 1993) may be a special case of the well-established pedestal effect known as the "transducer model" of flanker facilitation. In a typical pedestal experiment, the task of the observer is to detect a target super-imposed on a pedestal. If the target and the pedestal are the same in all spatiotemporal parameters except contrast, relative to the detection threshold measured with no pedestal, the target threshold first decreases (facilitation) and then increases as the pedestal contrast is increased (Chen & Foley, 2004; Foley, 1994; Foley & Chen, 1999; Kontsevich & Tyler, 1999a; Legge & Foley, 1980; Ross & Speed, 1991). Suppose that the receptive field of the detection mechanism is sufficiently large such that there is an overlap between the flankers and the receptive field when the flanker is close to the target. When the target receptive field completely overlaps with the flanker, the high contrast flanker has the same effect as a high contrast pedestal and has a masking effect on the target threshold. The overlap decreases with the distance between the flanker and the target. As a result, as the distance between the flanker and the target increases, the effect of a high contrast flanker is equivalent to a lower contrast pedestal. Thus, the target threshold decreases with flanker distance and shows a facilitation effect before returning to the level of the absolute detection threshold. That is, the flanker distance effect (Figure 5) corresponds to a TvC function plotted backward.

In this study, our measurements include both the TvC functions measured with no flanker presented and the flanker distance effect functions with no pedestal presented. Thus, we are able to test the reversed TvC function hypothesis with minimum extra assumptions. The red

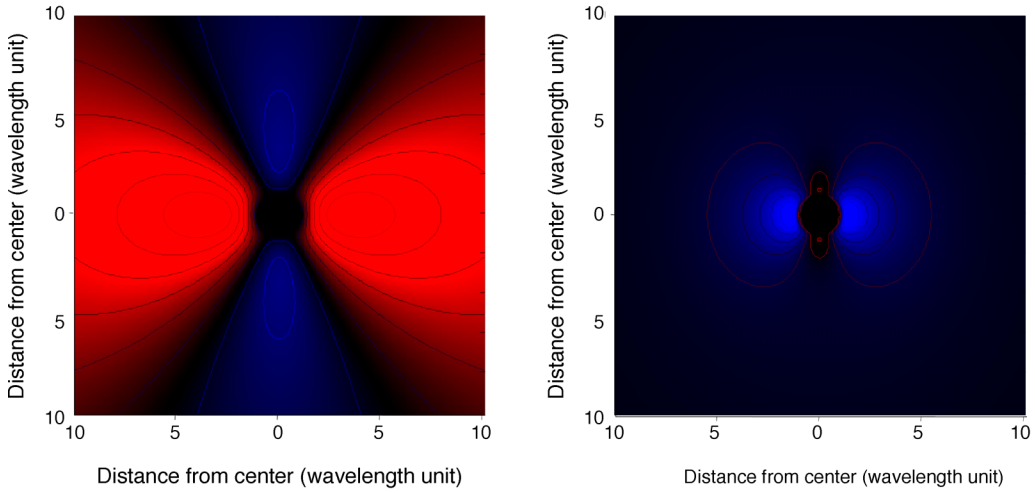

Figure 9. Estimated non-classical receptive field at target contrasts of 5% (left panel) and 50% (right panel) from the average values of the model fits for our observers from Figures 8 and 9. Red patches denote excitatory regions, and blue patches denote inhibitory.

curves in Figure 10 show the TvC function prediction of the flanker distance effect. We estimated the response of the target mechanism to the flanker alone and the flanker plus target from Equation 4. All the parameters, except the sensitivity to the flankers, were taken from the fit to the TvC functions. The sensitivity to the flankers, which depended on the size of the receptive field of the target mechanism, was derived from Equation 2 with the assumption that the receptive field can be described by a Gabor function. That is, the sensitivity to the flanker is

$$\mathrm{Se}_f = \mathrm{Se}_t * ((s^2 * \sigma^2)/(s^2 + \sigma^2))^{1/2} * \exp(-0.5 * u_y^2/(s^2 + \sigma^2)), \quad (12)$$

where σ is the scale parameter, u_y is the distance between the flanker and the target as discussed in the Methods section, and s is the scale parameter of the underlying receptive field and was the only extra free parameter to be estimated. It is obvious that the best TvC prediction fits the data poorly for all three observers (Figure 10, red curves). It predicts a much narrower range of facilitation (1–2 wavelength units) than the data shown (extending over ~6 wavelength units).

It may be argued that the target detector may not be the same for every flanker. It is likely that some off-center detector may produce greater differential responses between the flanker alone and the flanker plus target and thus determine the threshold. Such off-peak looking will indeed predict a slightly wider range of facilitation. To implement the off-peak looking prediction, we considered both the location of the detectors and the size of the detectors. Thus, the sensitivities of a target detector to the target and the flanker are defined as

$$\mathrm{Se}_t' = \mathrm{Se}_t * ((s^2 * \sigma^2)/(s^2 + \sigma^2))^{1/2} * \exp(-0.5 * u_t^2/(s^2 + \sigma^2)) \quad (13)$$

and

$$\mathrm{Se}_m' = \mathrm{Se}_t * ((s^2 * \sigma^2)/(s^2 + \sigma^2))^{1/2} * \exp(-0.5 * (u_t - u_m)^2 / (s^2 + \sigma^2)), \quad (14)$$

where Se_t' and Se_m' are the sensitivities of the off-peak linear filter to the target and to the nearby flankers, respectively, and u_t and u_m are the distances between the center of the off-peak linear filter to the target and the nearby flanker respectively. The sum of u_t and u_m is the distance between the flanker and the target. We then fit this off-peak model to the data (green dashed curves in Figure 10). Even with two extra parameters, u_t and s, there is no improvement in the qualitative fit to the data and is still a gross mismatch with the form of the flanker distance function. It is important to stress that any attempt to account for the spatial interaction function in terms of the TvC function needs to be assessed by such a quantitative modeling procedure, and that any such explanation is likely to fail if the range of spatial interactions are very different for the masking and facilitatory regions of the function.

The above analysis assumes an optimal receptive field size for the target detector. One may postulate that target detection may involve detectors of different sizes. As the flanker distance increases, there may always be a detector whose receptive field completely covers the flankers. While this model may maintain a flanker effect in the receptive field of the target detector, it cannot produce flanker facilitation at larger flanker distances. As the receptive field size increases, the target overlaps a smaller proportion of the receptive field. As a result, detectors with larger receptive fields are less sensitive to the target than those with smaller receptive fields. Hence, the threshold would be determined by the detector with the

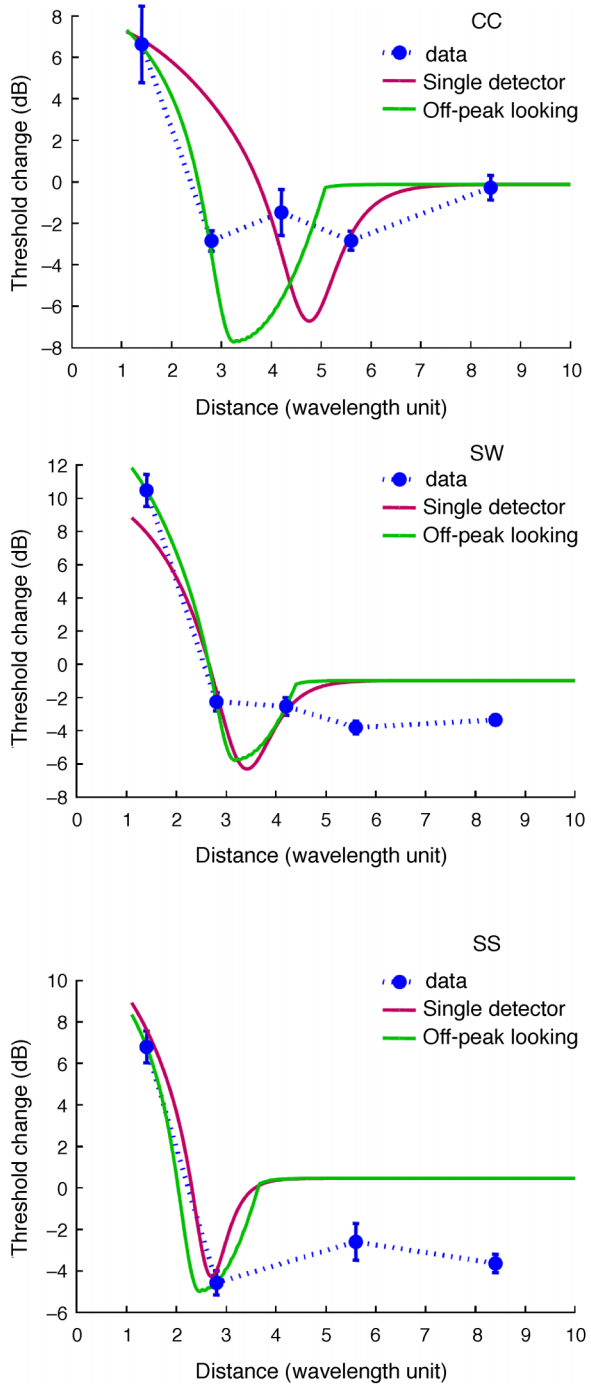

Figure 10. Flanker distance effect estimated from TvC functions. The red solid curves assume that the target threshold is determined by the one detector most sensitive to the target. The green dashed curves allow for off-peak detectors and assume that the threshold is determined by the detector with greatest difference between flanker only and flanker + target responses. The small discrepancy between the asymptotic level of the fits and 0 dB reflects the same discrepancy in the no-flanker condition, as shown in Figures 2 and 4.

optimal receptive field size and the model prediction will still be the same as those shown in Figure 10. The presence of an accelerating non-linearity at low contrasts will not help either because the large receptive fields are also less sensitive to the flankers and hence have less than optimal flanker effect.

A further strategy is to postulate that the gain increases with receptive field size and hence compensates the decrease in the overlap region between the target and the receptive field. Such mechanisms, however, contradict known empirical evidence. Chen and Tyler (1999) measured the foveal detection threshold to a string of up to eight Gabor patches. There was no significant threshold reduction for strings with more than two Gabor patches for either in-phase and alternating phase Gabor strings, indicating that there are no foveal detection mechanisms longer than 3λ. (Conversely, the results showed continuous summation up to 6λ for peripheral detection sites, but that performance is not relevant to this study.) Thus, a multiple size model cannot explain the data in Figure 10 either.

In addition to the distance effect, the transducer model also makes a prediction on how the TvC function should change with the presence of collinear flankers. In most conventional models for the TvC function, the inter-mechanism interaction is implemented in the pooling of the divisive inhibition signals (Equation 5). The presence of flankers only adds another term in the pooling process. Hence, as the flanker contrast was constant during the TvC measurement, its effect must be constant in the response function. As the pedestal contrast increases, the relative contribution of the flankers, compared with of the pedestal, becomes less significant at high pedestal contrasts than at low pedestal contrasts. As a result, the TvC function in the presence of the flankers should converge to the TvC function without flankers as pedestal contrast increases. This prediction is inconsistent with the data (Figures 2 and 4). In addition to the reduction of thresholds at low pedestal contrast, when an optimal flanker (e.g., collinear and at 3 wavelength distance) is presented, the TvC function actually shifted horizontally to the left on log-log coordinates. There is no sign of convergence between the TvC functions measured with and without flankers. This horizontal shift, however, is readily explained by our sensitivity modulation model (Figure 6). In our model, the presence of flankers changes the *sensitivity* of the target mechanism. The effect of the flanker is to multiply the response function by a factor (which will be an additive constant in logarithmic coordinates). When this effect is played through the generation of the TvC function, the flanker effect is to shift the high contrast portion of the TvC function horizontally to the left on a log–log plot. A detail analysis of the flanker effect of the shape of the TvC function was provided in Chen and Tyler (2001).

In summary, the failure of the pedestal-masking prediction in Figure 10 and the inconsistency between the data in Figures 2 and 4 and the prediction of the

models for pedestal effects lead us to conclude that the pedestal effect and the flanker effect are mediated by different mechanisms.

Uncertainty reduction interpretation of flanker effects

Recently, it was suggested that the flanker facilitation effect may be a result of uncertainty reduction (Petrov, Verghese, & McKee, 2006). That is, the presence of collinear flankers provides a cue to the exact position of the target and thus makes the target easier to detect when its position is otherwise uncertain. This theory cannot be used to explain our results, however. First, in our experiment, the task of an observer was to detect a target superimposed on a pedestal that occupied the same spatial location as the target. Such a pedestal effectively removes any uncertainty (Pelli, 1985) because the pooling mechanism must give the highest weight to the pedestal location where the target change occurs by virtue of its higher (pedestal) contrast. Thus, the presence of flankers cannot reduce uncertainty if there is no uncertainty in the first place. Second, the effect of uncertainty reduction is to decrease the threshold. Our data, however, showed that the presence of flankers *increased* threshold for high contrast pedestals. Third, the target was always placed halfway between the flankers. Hence, flankers in all the azimuths should provide the same cue about the location of the target and hence have the same uncertainty reduction. Yet, the detection threshold was modulated significantly (Figure 3) with flanker azimuth. In summary, for both theoretical and empirical reasons, our results cannot be explained by a reduction in uncertainty.

Conclusion

We measured contrast discrimination threshold in the presence of flankers that were either (i) collinear with the target and varying in distance or (ii) at a fixed distance from the target but with varying in location relative to the vertical axis. Compared with the no-flanker condition, the collinear flankers *decreased* target threshold at low pedestal contrasts (facilitation) and *increased* threshold at high contrasts (suppression). The low contrast facilitation increased with distance up to 4 wavelengths and decreased beyond that. Both facilitative and suppressive flanker effects were greatest at the collinear location and decreased monotonically as flanker location deviated from the collinear axis. This result reveals a spatial interaction field that is strongly dependent on the contrast at the target location. At low contrasts, the field of interaction on contrast discrimination is spatially extensive and is inhibitory for aligned flankers and facilitatory elsewhere. As contrast increases, the field of interactions shrinks and the configuration effects invert, becoming facilitatory for collinear flankers and inhibitory elsewhere. These effects cannot be explained in terms of the response properties of the classical receptive field, as represented by the transducer model based on the contrast discrimination function, but seem to be true spatial interactions corresponding to the non-classical receptive field recorded in cortical cells.

Acknowledgments

Supported by NSC 95-2752-H-002-006-PAE to CCC and NEI EY13025 to CWT.

Commercial relationships: none.
Corresponding author: Chien-Chung Chen.
Email: c3chen@ntu.edu.tw.
Address: Department of Psychology, National Taiwan University, Taipei 106, Taiwan.

References

Adini, Y., & Sagi, D. (2001). Recurrent networks in human visual cortex: Psychophysics evidence. *Journal of the Optical Society of America A, Optics, Image Science, and Vision, 18,* 2228–2236. [PubMed]

Breitmeyer, B. G. (1984). *Visual masking: An integrative approach*. Oxford: Oxford University Press.

Cavanaugh, J. R., Bair, W., & Movshon, J. A. (2002). Selectivity and spatial distribution of signals from the receptive field surround in macaque V1 neurons. *Journal of Neurophysiology, 88,* 2547–2556. [PubMed] [Article]

Chen, C. C., & Foley, J. M. (2004). Pattern detection: Interactions between oriented and concentric patterns. *Vision Research, 44,* 915–924. [PubMed]

Chen, C. C., Foley, J. M., & Brainard, D. H. (2000). Detection of chromoluminance patterns on chromoluminance pedestals: II. Model. *Vision Research, 40,* 789–803. [PubMed]

Chen, C. C., & Kasamatsu, T. (1998). A sensitivity modulation model for lateral interaction among striate cells in cat visual cortex. *Abstract of Society for Neuroscience, 24,* 1979.

Chen, C. C., Kasamatsu, T., Polat, U., & Norcia, A. M. (2001). Contrast response characteristics of long-range lateral interactions in cat striate cortex. *Neuroreport, 12,* 655–661. [PubMed]

Chen, C. C., & Tyler, C. W. (1999). Spatial pattern summation is phase-insensitive in the fovea but not in the periphery. *Spatial Vision, 12,* 267–285. [PubMed]

Chen, C. C., & Tyler, C. W. (2000). Spatial long-range modulation of contrast discrimination. *SPIE Proceedings, 4080,* 87–93.

Chen, C. C., & Tyler, C. W. (2001). Lateral sensitivity modulation explains the flanker effect in contrast discrimination. *Proceedings of the Royal Society of London B: Biological Sciences, 268,* 509–516. [PubMed] [Article]

Chen, C. C., & Tyler, C. W. (2002). Lateral modulation of contrast discrimination: Flanker orientation effects. *Journal of Vision, 2*(6):8, 520–530, http://journalofvision.org/2/6/8/, doi:10.1167/2.6.8. [PubMed] [Article]

Foley, J. M. (1994). Human luminance pattern-vision mechanisms: Masking experiments require a new model. *Journal of the Optical Society of America A, Optics, Image Science, and Vision, 11,* 1710–1719. [PubMed]

Foley, J. M., & Chen, C. C. (1999). Pattern detection in the presence of maskers that differ in spatial phase and temporal offset: Threshold measurements and a model. *Vision Research, 39,* 3855–3872. [PubMed]

Freeman, R. D., Ohzawa, I., & Walker, G. (2001). Beyond the classical receptive field in the visual cortex. *Progress in Brain Research, 134,* 157–170. [PubMed]

Heeger, D. J. (1992). Normalization of cell responses in cat striate cortex. *Visual Neuroscience, 9,* 181–197. [PubMed]

Kapadia, M. K., Westheimer, G., & Gilbert, C. D. (1999). Dynamics of spatial summation in primary visual cortex of alert monkeys. *Proceedings of the National Academy of Sciences of the United States of America, 96,* 12073–12078. [PubMed] [Article]

Kapadia, M. K., Westheimer, G., & Gilbert, C. D. (2000). Spatial distribution of contextual interactions in primary visual cortex and in visual perception. *Journal of Neurophysiology, 84,* 2048–2062. [PubMed] [Article]

Kontsevich, L. L., & Tyler, C. W. (1999a). Bayesian adaptive estimation of psychometric slope and threshold. *Vision Research, 39,* 2729–2737. [PubMed]

Kontsevich, L. L., & Tyler, C. W. (1999b). Nonlinearities of near-threshold contrast transduction. *Vision Research, 39,* 1869–1880. [PubMed]

Ledgeway, T., Hess, R. F., & Geisler, W. S. (2005). Grouping local orientation and direction signals to extract spatial contours: Empirical tests of "association field" models of contour integration. *Vision Research, 45,* 2511–2522. [PubMed]

Legge, G. E., & Foley, J. M. (1980). Contrast masking in human vision. *Journal of the Optical Society of America, 70,* 1458–1470. [PubMed]

Meese, T. S., & Holmes, D. J. (2007). Spatial and temporal dependencies of cross-orientation suppression in human vision. *Proceedings of the Royal Society of London B: Biological Sciences, 274,* 127–136. [PubMed] [Article]

Meese, T. S., Summers, R. J., Holmes, D. J., & Wallis, S. A. (2007). Contextual modulation involves suppression and facilitation from the center and the surround. *Journal of Vision, 7*(4):7, 1–21, http://journalofvision.org/7/4/7/, doi:10.1167/7.4.7. [PubMed] [Article]

Mizobe, K., Polat, U., Pettet, M. W., & Kasamatsu, T. (2001). Facilitation and suppression of single striate-cell activity by spatially discrete pattern stimuli presented beyond the receptive field. *Visual Neuroscience, 18,* 377–391. [PubMed]

Pelli, D. G. (1985). Uncertainty explains many aspects of visual contrast detection and discrimination. *Journal of the Optical Society of America A, 2,* 1508–1532. [PubMed]

Petrov, Y., Verghese, P., & McKee, S. P. (2006). Collinear facilitation is largely uncertainty reduction. *Journal of Vision, 6*(2):8, 170–178, http://journalofvision.org/6/2/8/, doi:10.1167/6.2.8. [PubMed] [Article]

Polat, U., & Sagi, D. (1993). Lateral interactions between spatial channels: Suppression and facilitation revealed by lateral masking experiments. *Vision Research, 33,* 993–999. [PubMed]

Polat, U., & Sagi, D. (1994). The architecture of perceptual spatial interactions. *Vision Research, 34,* 73–78. [PubMed]

Polat, U., Sagi, D., & Norcia, A. M. (1997). Abnormal long-range spatial interactions in amblyopia. *Vision Research, 37,* 737–744. [PubMed]

Ross, J., & Speed, H. D. (1991). Contrast adaptation and contrast masking in human vision. *Proceedings of the Royal Society of London B: Biological Sciences, 246,* 61–69. [PubMed]

Sengpiel, F., Baddeley, R. J., Freeman, T. C., Harrad, R., & Blakemore, C. (1998). Different mechanisms underlie three inhibitory phenomena in cat area 17. *Vision Research, 38,* 2067–2080. [PubMed]

Solomon, J. A., & Morgan, M. J. (2000). Facilitation from collinear flanks is cancelled by non-collinear flanks. *Vision Research, 40,* 279–286. [PubMed]

Solomon, J. A., Watson, A. B., & Morgan, M. J. (1999). Transducer model produces facilitation from opposite-sign flanks. *Vision Research, 39,* 987–992. [PubMed]

Teo, P. C., & Heeger, D. J. (1994). Perceptual image distortion. *SPIE Proceedings, 2179,* 127–141.

Tyler, C. W., & McBride, B. (1997). The Morphonome image psychophysics software and a calibrator foe Macintosh systems. *Spatial Vision, 10,* 479–484. [PubMed]

Watson, A. B., & Solomon, J. A. (1997). Model of visual contrast gain control and pattern masking. *Journal of the Optical Society of America A, Optics, Image Science, and Vision, 14,* 2379–2391. [PubMed]

Wilson, H. R., & Humanski, R. (1993). Spatial frequency adaptation and contrast gain control. *Vision Research, 33,* 1133–1149. [PubMed]

Wilson, H. R., McFarlane, D. K., & Philips, G. C. (1983). Spatial frequency tuning of orientation selectivity units estimated by oblique masking. *Vision Research, 23,* 873–882. [PubMed]

Xing, J., & Heeger, D. J. (2001). Measurement and modeling of center-surround suppression and enhancement. *Vision Research, 41,* 571–583. [PubMed]

Yu, C., Klein, S. A., & Levi, D. M. (2002). Facilitation of contrast detection by cross-oriented surround stimuli and its psychophysical mechanisms. *Journal of Vision, 2*(3):4, 243–255, http://journalofvision.org/2/3/4/, doi:10.1167/2.3.4. [PubMed] [Article]

Yu, C., Klein, S. A., & Levi, D. M. (2003). Cross- and iso-oriented surrounds modulate the contrast response function: The effect of surround contrast. *Journal of Vision, 3*(8):1, 527–540, http://journalofvision.org/3/8/1/, doi:10.1167/3.8.1. [PubMed] [Article]

Zenger, B., & Sagi, D. (1996). Isolating excitatory and inhibitory nonlinear spatial interactions involved in contrast detection. *Vision Research, 36,* 2497–2513. [PubMed]

Zenger-Landolt, B., & Koch, C. (2001). Flanker effects in peripheral contrast discrimination-psychophysics and modeling. *Vision Research, 41,* 3663–3775. [PubMed]